Superconducting nonequilibrium transport through a weakly interacting quantum dot

L. Dell'Anna, A. Zazunov, and R. Egger
Institut für Theoretische Physik, Heinrich-Heine-Universität, D-40225 Düsseldorf, Germany
(Received 11 January 2008; published 25 March 2008)

We study the out-of-equilibrium current through an interacting quantum dot, which is modeled as an Anderson impurity contacted by two BCS superconductors held at fixed voltage bias. In order to account for multiple Andreev reflections, we develop a Keldysh Green's function scheme perturbative in the dot's interaction strength. We find an unexpected enhancement of the current due to repulsive interactions for small to intermediate lead-to-dot couplings.

DOI: 10.1103/PhysRevB.77.104525 PACS number(s): 74.45.+c, 73.63.−b, 74.50.+r

I. INTRODUCTION

Superconducting transport through low-dimensional nanoscale structures is currently attracting considerable interest. Gate-tunable Josephson currents through nanowire-based quantum dots have been reported,[1] and similar setups have been realized using (short) carbon nanotubes[2,3] and metallofullerene molecules.[4] Nonequilibrium transport in such systems contacted by superconducting electrodes has been a particular focus of recent experimental effort,[3–9] which is mainly caused by an interesting interplay between interaction effects (on the quantum dot) and superconducting correlations (due to the electrodes). One remarkable consequence is the observation of an "even-odd" effect (as a function of the dot's occupation number) in the conductance.[8,9] This effect is presumably caused by the absence or presence of Kondo correlations. In this paper, we analyze superconducting transport through an interacting quantum dot for the simplest case of a single spin-degenerate level with repulsive on-site interaction energy $U>0$ (Anderson impurity), which is contacted by two wide s-wave BCS superconducting electrodes with identical gap Δ. For simplicity, we assume that both lead-to-dot couplings (hybridizations) are equal, i.e., $\Gamma_L=\Gamma_R=\Gamma$, and consider the two electrodes held at potential difference (voltage bias) V. By a systematic perturbative expansion in the interaction strength U, we compute the I-V characteristics, in particular, for the interesting subgap regime $eV<2\Delta$, where multiple Andreev reflection (MAR) processes provide the dominant transport mechanism. A theory of coherent MAR has been originally developed for superconducting point contacts,[10] with the essential assumption that charging interaction effects inside the contact can be neglected. The problem of resonant MAR through a noninteracting quantum level has been treated in Refs. 11–13.

While the interacting problem in equilibrium has been theoretically studied by many authors,[14] the corresponding nonequilibrium problem is more difficult and far less understood. Previous approaches can be broadly grouped in three classes. (i) By ignoring MAR processes in the Coulomb blockade regime, additional side peaks in the differential conductance at $eV=2\Delta$ and $2(\Delta+U)$ were predicted,[15] which reflects the singularity of the BCS spectral density of the leads. (ii) Different mean-field schemes have been proposed,[12,16,17] which are based on slave-boson or Hubbard–Stratonovich-path-integral approaches. These calculations predict an overall suppression of the current by the interactions. This suppression is obtained only for sufficiently repulsive interactions, while there is no interaction effect for weak interaction.[16] (iii) A Fermi liquid approach valid in the deep Kondo limit has been proposed.[18] Here, we do not discuss the Kondo regime but instead focus on the limit of weak interactions, $U/\Gamma<1$, where a controlled perturbative expansion in the small parameter U/Γ is possible. Note that this approach still allows for arbitrary ratio Γ/Δ. Such calculations have been carried out for normal-conducting ($\Delta=0$) electrodes recently,[19–21] and we here generalize them to superconducting electrodes. The case $U<\Gamma$ is of experimental relevance for the understanding of superconducting transport through quantum dots or molecules with good lead-to-dot couplings.

The structure of the remainder of this paper is as follows. In Sec. II, we discuss our perturbation theory approach to superconducting transport through an Anderson dot and its numerical implementation. Results for the current-voltage characteristics are shown and discussed in Sec. III. The appendix contains qualitative arguments for the current enhancement found at $\Gamma<\Delta$, which is based on an evaluation of the Josephson current. We often set $\hbar=e=1$.

II. PERTURBATIVE APPROACH TO SUPERCONDUCTING TRANSPORT

We consider the canonical Anderson impurity model, $H=H_D+H_T+H_L+H_R$, where a single-level dot with spinful fermion d_σ (H_D) is tunnel coupled (H_T) to left and right superconducting reservoirs $H_{L/R}$ held at chemical potential difference eV. The isolated dot corresponds to ($n_\sigma=d_\sigma^\dagger d_\sigma=0,1$)

$$H_D=E_0(n_\uparrow+n_\downarrow)+Un_\uparrow n_\downarrow=\epsilon_0(n_\uparrow+n_\downarrow)-\frac{U}{2}(n_\uparrow-n_\downarrow)^2. \tag{1}$$

The "noninteracting" model below is taken to contain the interaction level shift $\epsilon_0=E_0+U/2$ of the bare level E_0. The leads are described by a pair of s-wave BCS Hamiltonians in the standard wide-band limit. We are interested in the $V\neq 0$ case and take the same real-valued gap parameter $\Delta>0$ for both electrodes. By using the Nambu vector $\Psi_{j,k}^T=(\psi_{j,k,\uparrow},\psi_{j,-k,\downarrow}^\dagger)$ for electrons in lead $j=L/R$, we thus have (we set $\hbar=e=1$ in intermediate steps)

$$H_j = \sum_k \Psi_{jk}^\dagger [(k^2/2m - \epsilon_F)\sigma_z + \Delta\sigma_x]\Psi_{jk}, \tag{2}$$

with Pauli matrices σ_i (τ_i) in Nambu (Keldysh) space. By using the Nambu vector $d=(d_\uparrow, d_\downarrow^\dagger)^T$ and $\Gamma=\pi\nu_0|t_0|^2$ for (normal) lead density of states ν_0, the lead-dot coupling is

$$H_T = t_0 \sum_{k,j=L/R=\pm} \Psi_{jk}^\dagger \sigma_z e^{\pm i\sigma_z Vt/2} d + \text{H.c.}, \tag{3}$$

where the voltage V enters via the time-dependent phase. We now define the Keldysh–Nambu Green's function for the dot fermions as

$$G_{\alpha\alpha'}^{ss'}(t,t') = -i\langle \hat{T}_C[d_\alpha(t_s)d_{\alpha'}^\dagger(t_{s'})]\rangle, \tag{4}$$

where $\alpha,\alpha'=1,2$ $(s,s'=1,2)$ are Nambu (Keldysh) indices and $\hat{T}_C$ is the time-ordering operator along the Keldysh contour. Accordingly, t_s denotes a time taken on branch s of the Keldysh contour. It is convenient to use the Fourier decomposition as[22]

$$G^{ab}(t,t') = \sum_{n,m=-\infty}^{\infty} \int_F \frac{d\omega}{2\pi} e^{-i\omega_n t + i\omega_m t'} G_{nm}^{ab}(\omega), \tag{5}$$

where $a,b=1,\ldots,4$ denotes the Nambu–Keldysh indices defined by $a=\alpha+2(s-1)$ and $\omega_n=\omega+nV$ for ω within the "fundamental" domain $F\equiv[-V/2,V/2]$. For fixed $\omega\in F$, the Dyson equation for the full Green's function $\check{G}$ (the inverted caret refers to the Keldysh–Nambu structure),

$$\check{G}^{-1} = \check{G}_0^{-1} - \check{\Sigma}, \tag{6}$$

then becomes a matrix equation suitable for numerical inversion. Here, interaction effects are encoded in the self-energy $\check{\Sigma}$. After integrating out the lead fermion degrees of freedom, the noninteracting Green's function $\check{G}_0$ is

$$\check{G}_{0,nm}^{-1}(\omega) = (\omega_n - \epsilon_0\sigma_z)\tau_z\delta_{nm} - \Gamma\sum_{j=L/R}\check{\gamma}_{j,nm}(\omega). \tag{7}$$

The self-energy due to tracing out the respective lead is given by the Nambu matrix as

$$\check{\gamma}_{j=L/R=\pm,nm}(\omega) = \begin{pmatrix} \delta_{nm}\check{X}(\omega_n \mp V/2) & \delta_{m,n\mp1}\check{Y}(\omega_n \mp V/2) \\ \delta_{m,n\pm1}\check{Y}(\omega_n \pm V/2) & \delta_{nm}\check{X}(\omega_n \pm V/2) \end{pmatrix}, \tag{8}$$

with Keldysh matrices $\check{Y}(\omega)=-\Delta\check{X}(\omega)/\omega$ and

$$\check{X}(\omega) = \begin{cases} -\dfrac{\omega}{\sqrt{\Delta^2-\omega^2}}\tau_z, & |\omega|<\Delta \\ \dfrac{i|\omega|}{\sqrt{\omega^2-\Delta^2}}\begin{pmatrix} 2f_\omega - 1 & -2f_\omega \\ 2f_{-\omega} & 2f_\omega - 1 \end{pmatrix}, & |\omega|>\Delta \end{cases},$$

where $f_\omega=1/(1+e^{\omega/k_BT})$ is the Fermi function. The steady-state dc current through the left and/or right junction then follows as

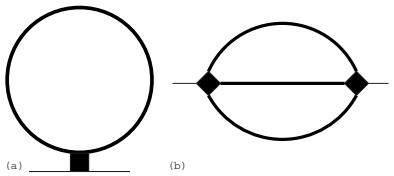

FIG. 1. Electron-electron interaction self-energy diagrams taken into account in this paper: (a) first order (left) and (b) second order (right).

$$I_{L/R} = \mp 2\Gamma\ \text{Re}\sum_{nm}\int_F \frac{d\omega}{2\pi}\text{tr}[\sigma_z\check{\gamma}_{L/R,nm}(\omega)\check{G}_{mn}(\omega)]^{+-}, \tag{9}$$

where the trace is only over the Nambu space and (+−) refers to the (12) Keldysh component. Current conservation, $I_L=I_R=I$, is fulfilled for all results below.

A. First order

Since the exact self-energy $\check{\Sigma}$ is not known, we proceed in a perturbative fashion, starting with the first-order self-energy in Fig. 1(a), which is made self-consistent by using the full $\check{G}$ in the diagram. It is convenient to introduce the four-point vertex (cf. also Ref. 19),

$$\Lambda_{abcd} = \frac{1}{2}(\delta_{ab}\tau_{cd} + \delta_{cd}\tau_{ab} - \delta_{ad}\tau_{cb} - \delta_{cb}\tau_{ad}), \tag{10}$$

where $\tau=\sigma_0\tau_z=\text{diag}(1,1,-1,-1)$. Only eight out of the possible 256 entries of the tensor Λ are nonzero, with values ±1. With this convention, the complete first-order self-energy is given by

$$\Sigma_{n,n+m}^{(1)ab} = iU\Lambda_{abcd}\sum_{n'}\int_F \frac{d\omega'}{2\pi}G_{n',n'+m}^{dc}(\omega'), \tag{11}$$

where we use the sum convention for c and d. Note that this self-energy is independent of (n,ω) but still depends on the "off-diagonal" frequency index m. In time representation, $m\neq0$ contributions come with phase factors $e^{\pm 2imVt}$ and thus correspond to anomalous (pairing) correlations. The presence of the off-diagonal harmonics in the self-energy is a consequence of the coherent MAR transport regime considered here. The role of coherence is particularly important for the interplay between MAR processes and charging effects in a quantum dot with a relatively strong coupling to the leads.

At that stage, let us briefly compare the first-order self-consistent approach based on Eqs. (6) and (11) to the mean-field approximation of Ref. 16. The latter effectively considers only the time averaged components of the self-energy [Eq. (11)] corresponding to the two first terms of Eq. (10), thereby discarding all harmonics with $m\neq0$ and exchange terms in Eq. (11). The resulting self-energy contributions, which are taken into account in Ref. 16, correspond to $\gamma_+\tau_0$ and $\gamma_-\tau_z$. The scalar constants $\gamma_\pm$ can be written as

$$\gamma_+ = i\frac{U}{2}\sum_{n'}\int_F \frac{d\omega'}{2\pi}\text{Tr}[\tau_z\check{G}_{n'n'}(\omega')],$$

$$\gamma_- = i\frac{U}{2}\sum_{n'}\int_F \frac{d\omega'}{2\pi}\mathrm{Tr}[\check{G}_{n'n'}(\omega')], \tag{12}$$

where the trace is over both the Nambu and Keldysh spaces. Under this approximation, there is no interaction effect on the current $I(V)$ below some critical value U_c. In fact, nontrivial stable solutions $\gamma_\pm \neq 0$ for the self-consistency equation [Eq. (12)] exist only for $U > U_c$,[16] where U_c depends on V, Γ, and Δ. The symmetry-broken phase with $\gamma_- \neq 0$ corresponds to a spin-polarized dot, and one then finds a Coulomb blockade suppression of the current.[16] However, for normal leads, serious problems with spin-polarized out-of-equilibrium mean-field solutions for the Anderson dot have been recently identified,[23] and those arguments also apply to the superconducting case. A typical value is $U_c \approx \Gamma$ for $V \approx \Gamma \approx \Delta/2$, and we shall always limit ourselves to $U < U_c$ where no such problems arise. In our calculations, the actual value of U_c follows from the numerical solution of the self-consistency problem, and we can thereby ensure that no spin-polarized solutions are present. In contrast to the mean-field scheme of Ref. 16, however, the full first-order self-consistent approach generates sizeable interaction corrections even for small U (see Sec. III). These corrections are not just a matter of numerical accuracy but reflect the importance of on-dot pairing terms.

B. Second order

To go beyond the self-consistent first-order approximation given by Eq. (11), we have to evaluate the second-order diagram, as shown in Fig. 1(b). Due to the large numerical effort in evaluating this diagram, we restrict ourselves to a non-self-consistent scheme at this point, i.e., we use the solution $\check{G}$ of the first-order problem to evaluate $\check{\Sigma}^{(2)}$. As is well known,[24,25] under such a scheme, current conservation is only ensured for the particle-hole symmetric case, i.e., $\epsilon_0 = 0$ (see also Ref. 22). We therefore show second-order results only for $\epsilon_0 = 0$. The second-order Nambu–Keldysh self-energy in time representation reads (sum convention)

$$\Sigma^{(2)ab}(t,t') = \frac{U^2}{2}\Lambda_{afgh}\Lambda_{ebcd}G^{fe}(t,t')G^{dg}(t',t)G^{hc}(t,t'). \tag{13}$$

To avoid numerically expensive frequency convolutions, it is convenient to first compute the Green's function in time representation according to Eq. (5), then evaluate the self-energy in Eq. (13), and finally, transform this result back to frequency space to use it in the Dyson equation [Eq. (6)]. Notice that Eq. (13), which corresponds to the skeleton diagram in Fig. 1(b), represents only a part of all possible second-order contributions. The rest is given by the time-local piece,

$$-U^2\Lambda_{abcd}\Lambda_{efgh}\int dt'' G^{de}(t,t'')G^{hg}(t'',t'')G^{fc}(t'',t),$$

which has already been taken into account by our self-consistent first-order solution.

C. Calculation of current

The numerical implementation of the above perturbative approach is straightforward. To evaluate the current $I(V)$ from Eq. (9), we partition the frequency summations into windows of width V and impose a bandwidth cutoff ω_c, such that $|\omega_n| < \omega_c$. In our calculations, we use $\omega_c = 10\Delta$, but the precise choice is not critical. We then discretize the fundamental frequency domain F with a step size $\delta\omega$ and use a fast Fourier transform routine to switch between time and frequency representations. (The efficient evaluation of the second-order self-energy requires to employ the time representation, while the Dyson equation needs the frequency representation.) Typically, we found $\delta\omega = 0.005\Delta$ to be sufficient for convergence. The matrix inversion in Eq. (6) is then separately performed for each $\omega \in F$ involving matrix dimensions of the order of $\omega_c/|V|$. We refer to Ref. 22 for further details of the numerical implementation in the related case of a phonon-mediated interaction.

In a first step, we solve the first-order self-consistent problem posed by Eqs. (6), (7), and (11). This solution proceeds iteratively, where the stability or instability of the solution for $\check{G}$ is carefully checked by probing small deviations around it. The iterative solution can, in fact, be carried out with very modest computational effort and quickly converges to a unique solution (as long as $U < U_c$). In a second step, we then use this converged first-order Green's function to evaluate $\check{\Sigma}^{(2)}$ according to Eq. (13) and to finally compute the current from Eq. (9). The second-order calculation is quite time consuming for low bias voltage, where many MAR orders need to be taken into account, and we therefore restricted our calculations to $eV/\Delta \geq 0.2$. As a consistency check for our numerical code, we have reproduced known results for $U=0$ (see Refs. 11–13) and the corresponding perturbative-in-U results for normal-conducting leads ($\Delta = 0$) (see Refs. 19 and 20). We have also reproduced the respective results of Ref. 16 when implementing their approximations. As an additional check, the Green's function sum rules, such as $\mathrm{tr}[\tau_z\sigma_z\check{G}(t,t)] = 0$ at coinciding times, have been verified.

III. RESULTS AND DISCUSSION

Next, we discuss numerical results obtained under the perturbative approach, as described in Sec. II. All results are for $T=0$, and unless noted otherwise, we set $U/\Gamma = 0.5$ which is sufficiently small to ensure $U < U_c$ for all investigated V/Δ and Γ/Δ but large enough to produce significant interaction corrections to the I-V characteristics. We will focus on the most interesting subgap regime, i.e., $eV < 2\Delta$. The excess current $I_{exc} = \lim_{V\to\infty}[I(V,\Delta) - I(V,\Delta=0)]$ has also been computed. The interaction contribution δI_{exc} to this quantity turns out to be generally small, which is similar to what is found for the case of phonon-mediated interactions.[22] Remarkably, this interaction correction is positive for $\Gamma \lesssim \Delta$, which points toward a current enhancement. This trend is quite generic and discussed next.

Let us start by showing results obtained from the first-order self-consistent scheme (i.e., without the second-order self-energy). In that case, by virtue of self-consistency, we

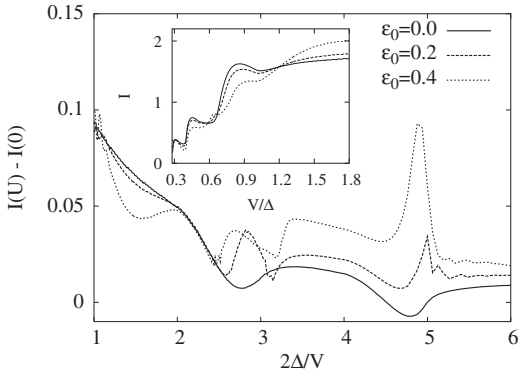

FIG. 2. Interaction correction to the current (currents are always plotted in units of $e\Delta/h$) from the self-consistent first-order approach for $U/\Gamma=\Gamma/\Delta=0.5$ and various ϵ_0/Δ. The inverse voltage scale is taken to compare with standard MAR features. Inset: Full *I-V* curves for same parameters.

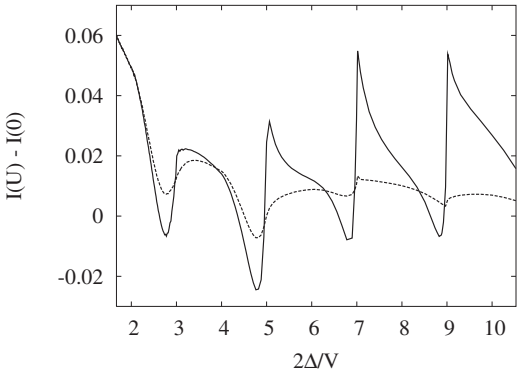

FIG. 3. Same as Fig. 2 but for $\epsilon_0=0$. The dashed curve gives the first-order self-consistent result, while the solid curve includes also the second-order contribution.

have the freedom to vary ϵ_0 without spoiling current conservation.[24,25] Representative numerical results for the voltage-dependent interaction correction to the current, $I(U)-I(U=0)$, are shown for $\Gamma/\Delta=0.5$ in Fig. 2. For all results shown here, we have $U<U_c$, and the approach of Ref. 16 would not yield any interaction correction. However, we find significant interaction effects for $U<U_c$ within the full first-order self-consistent approach. These effects are due to the time-dependent ($m\neq 0$) parts of the self-energy [Eq. (11)], which contain pairing order parameters on the dot. For instance, at the symmetric point $\epsilon_0=0$, we find by perturbation theory in U that $\gamma_{\pm}=0$, but the complex-valued $m=1$ pairing term

$$\delta \equiv \Sigma_{n,n+1}^{(1),12} \tag{14}$$

stays finite. This ω-independent off-diagonal Nambu component of the self-energy, which is absent in the normal ($\Delta=0$) case, describes the effect of interactions on the proximity-induced pairing correlation on the dot. At the mean-field level, γ_- is dominant for large U, while terms such as δ dominate for small U. Similar contributions with $|m|>1$ exist and are kept in our self-consistent first-order calculations, but they turn out to be significantly smaller.

Quite remarkably, we find $I(U)>I(U=0)$ for most voltages and/or dot level energies ϵ_0, which point to an *enhancement of the MAR-mediated current by repulsive interactions*. We have persistently found this unexpected feature throughout the parameter regime $\Gamma<\Delta$ and also when including the second-order self-energy (see below). A similar (but weaker) enhancement can be analytically found for the critical Josephson current of this system in equilibrium (see the Appendix). The current enhancement is reminiscent yet different from the "antiblockade" behavior due to dynamical Coulomb blockade effects on MAR transport, as discussed in Ref. 26. It is also consistent with the crossover from current enhancement to decrease with growing Γ for phonon-mediated interactions and normal-conducting leads.[21]

To illustrate the role of the second-order contribution for $U/\Gamma=0.5$, we now focus on the symmetric case $\epsilon_0=0$ by first taking again $\Gamma/\Delta=0.5$. The results of the first- and second-order calculations are compared in Fig. 3. Notice that the second-order correction, which is the leading time-nonlocal term in the perturbative expansion, becomes more and more important when lowering the voltage. In agreement with the conclusion drawn from the first-order self-consistent calculation, as shown in Fig. 2, a clear enhancement of the current by interactions can be observed for a broad range of voltages. This enhancement is especially pronounced for voltages slightly below the odd MAR peaks located at $eV=2\Delta/(2n+1)$. As indicated by our results for larger Γ (see Fig. 4 for the case $\Gamma/\Delta=2$), the interaction-induced enhancement of the current is restricted to small Γ/Δ. For larger Γ/Δ, the current instead is weakly suppressed by interactions. The same pronounced MAR peak structure, as in Fig. 3, can be observed in the pair order parameter δ defined in Eq. (14), whose absolute value is shown in Fig. 5. The fact that the characteristic MAR features still appear at $eV=2\Delta/n$ for the interacting case indicates that, at least for small U, the number of Andreev reflections is not affected by the Coulomb interaction. This is in contrast to the inelastic MAR picture for phonon-mediated interactions, as discussed in Ref. 22. Moreover, our results indicate that the Andreev quasiresonances[11,13] are not shifted away from the gap subharmonics.

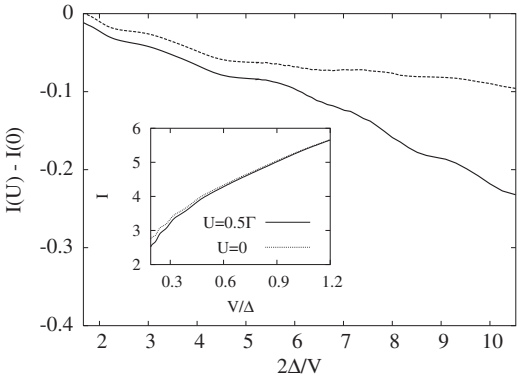

FIG. 4. Same as Fig. 3 but for $\Gamma=2\Delta$. Inset: *I-V* curve from second-order perturbation theory and for $U=0$.

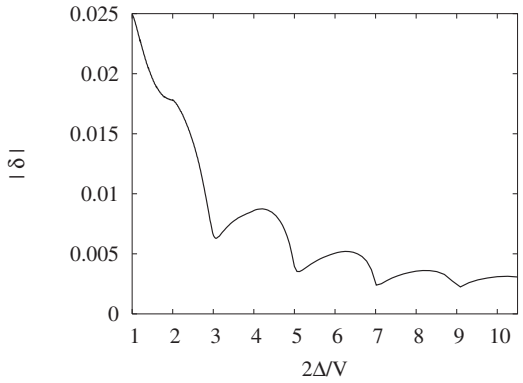

FIG. 5. Absolute value of δ [see Eq. (14)] in units of Δ for the parameters in Fig. 3.

As follows from our numerical analysis, the magnitude of the difference current is mainly determined by the first harmonics of interaction-mediated pairing [Eq. (14)] and can be roughly approximated as

$$I(U) - I(0) \sim (e/\hbar)|\delta|\Delta/\Gamma. \tag{15}$$

This can be seen, for instance, from a comparison of the curves in Figs. 5 and 2 (for $\epsilon_0=0$). A similar expression for the difference current [Eq. (15)] is also obtained from a simple Fermi golden rule calculation by analyzing the dynamics of Andreev (subgap) states at very low voltages, $eV \ll \Delta$. The corresponding correction to the transition rate from Andreev states into the continuum is determined by the imaginary part of the Andreev state self-energy $\Sigma_A(\omega) = \delta\sqrt{\Delta^2-\omega^2}/\Gamma$, while the total escape probability leading to the difference current is given by an expression similar to Eq. (3) in Ref. 18.

The above results also suggest that as a function of the ratio Γ/Δ, there should be a crossover from enhancement to suppression of the current around $\Gamma/\Delta \approx 1$. This is what we get when fixing the voltage and changing Γ/Δ. In Fig. 6, we have chosen $V=0.6\Delta$, where the self-consistent first-order approximation gives the main contribution, and plotted $I(U)-I(0)$ either for fixed $U/\Gamma=0.5$ (solid line) or for fixed $U/\Delta=0.25$ (dashed line). The two curves both cross zero approximately at the same value, $\Gamma \simeq \Delta$.

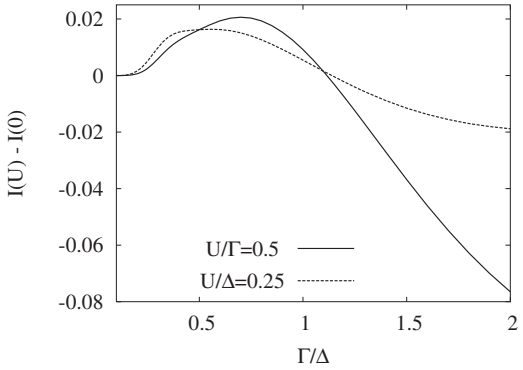

FIG. 6. $I(U)$-$I(0)$ vs Γ/Δ at $V=0.6\Delta$, $\epsilon_0=0$, fixing $U/\Gamma=0.5$ (solid line) or $U/\Delta=0.25$ (dashed line) from self-consistent first-order perturbation theory.

In conclusion, we have presented a theory which explores the effect of weak interactions on superconducting transport through a quantum dot. By employing second-order perturbation theory, which is valid for $U<\Gamma$, we find an unexpected enhancement of the subgap current against its noninteracting value when the hybridization Γ is smaller than the BCS gap parameter Δ. The perturbation theory scheme that is pursued in this paper offers controlled results in one corner of the parameter regime, and in contrast to previous mean-field theories, we predict significant interaction corrections even for weak interactions.

ACKNOWLEDGMENTS

We thank A. L. Yeyati, T. Martin, and V. Shumeiko for discussions. This work was supported by the EU HYSWITCH and INSTANS networks.

APPENDIX: JOSEPHSON CURRENT

In this appendix, we briefly show that the interaction-induced current enhancement found in the I-V curves for $\Gamma < \Delta$, as discussed in Sec. III, also appears in the equilibrium Josephson current-phase relation (where ϕ is the phase difference across the dot) for the same model. We consider the corresponding first-order self-consistent theory in equilibrium, for simplicity, at $\epsilon_0=0$ only. For small U, no polarization is present, $\gamma=0$, and only the proximity-induced mean-field parameter $\delta = U\langle d_\uparrow^\dagger d_\downarrow^\dagger\rangle$ gives an effect. Assuming real-valued δ, the $T=0$ self-consistency equation reads

$$\delta = U\int_{-\infty}^{\infty}\frac{d\omega}{2\pi}\frac{\beta_\omega-\delta}{\alpha_\omega^2+(\beta_\omega-\delta)^2}, \tag{A1}$$

where

$$\alpha_\omega = \omega\left(1+\frac{\Gamma}{\sqrt{\omega^2+\Delta^2}}\right), \quad \beta_\omega = \frac{\Gamma\Delta\cos(\phi/2)}{\sqrt{\omega^2+\Delta^2}}.$$

The Josephson current is then given as

$$I = \frac{e\Gamma\Delta}{\pi\hbar}\sin(\phi/2)\int_{-\infty}^{\infty}\frac{d\omega}{\sqrt{\omega^2+\Delta^2}}\frac{\beta_\omega-\delta}{\alpha_\omega^2+(\beta_\omega-\delta)^2}. \tag{A2}$$

The presence of δ in Eq. (A2) generally causes two counteracting effects: There is a decrease in I due to the numerator but an increase due to the appearance of δ in the denominator. Which of these is more important can only be clarified by detailed calculation. We present analytical evaluations valid for $|\delta| \ll \Gamma|\cos(\phi/2)|$ separately for the regimes $\Gamma/\Delta \ll 1$ and $\Gamma/\Delta \gg 1$.

Let us first discuss $\Gamma/\Delta \ll 1$, where Eq. (A1) yields

$$\frac{\delta}{U} \simeq \frac{\Delta}{2|\Gamma\cos(\phi/2)-\delta|} \times\left(\frac{2\Gamma\cos(\phi/2)\cos^{-1}\left|\frac{\Gamma\cos(\phi/2)-\delta}{\Delta}\right|}{\pi\sqrt{\Delta^2-[\Gamma\cos(\phi/2)-\delta]^2}}-\frac{\delta}{\Delta}\right). \tag{A3}$$

The interaction correction to the Josephson current now follows from Eq. (A2),

$$\delta I \simeq \frac{2e\delta}{\hbar}\tan(\phi/2)\left(\frac{1}{2}f_1(\phi)\mathrm{sgn}\cos(\phi/2)-\frac{\delta}{U}\right).$$

with

$$f_1(\phi)=\frac{1+2(\Gamma/\Delta)|\cos(\phi/2)|}{[1+(\Gamma/\Delta)|\cos(\phi/2)|]^2}=1+O(\Gamma^2/\Delta^2).$$

In the extreme limit $\Gamma/\Delta\to 0$, Eq. (A3) yields $\delta=(U/2)\mathrm{sgn}\cos(\phi/2)$, and then, $\delta I=0$. An inspection of Eq. (A3) for finite $\Gamma/\Delta\ll 1$ shows, however, that $|\delta|<U/2$ for $\phi\neq\pi$. As a result, the interaction current to the Josephson current for $\Gamma\ll\Delta$ turns out to be positive, although it is numerically small. Using Eq. (A3), we find

$$\delta I \simeq \frac{eU}{\hbar\pi}\frac{\Gamma}{\Delta}\sin(\phi/2)\mathrm{sgn}\cos(\phi/2).$$

We believe that this effect is related to the enhancement of the current at finite bias V in the regime $\Gamma\ll\Delta$, as discussed in Sec. III.

On the other hand, for $\Gamma\gg\Delta$, Eq. (A1) is solved by $\delta\simeq U\Delta\ln(\Gamma/\Delta)\cos(\phi/2)/(\pi\Gamma)$, and the lowest-order interaction correction to the Josephson current is

$$\delta I \simeq \frac{2e\delta}{\hbar}\tan(\phi/2)\left(\frac{\Delta}{2\Gamma}f_2(\phi)\mathrm{sgn}\cos(\phi/2)-\frac{\delta}{U}\right),$$

with $f_2(\phi)=1+\cos^2(\phi/2)/4$. Due to the large $\ln(\Gamma/\Delta)$ factor appearing now in δ, the Josephson current will, in general, be decreased by interactions for $\Gamma\gg\Delta$.

We therefore find the same qualitative picture as for the nonequilibrium current in Sec. III: The equilibrium Josephson current can also be slightly increased by weak repulsive interactions for weak hybridization, $\Gamma/\Delta\ll 1$, but is decreased in the opposite limit. However, the increase in the Josephson current for weak hybridization turns out to be much smaller than for the corresponding nonequilibrium current.

[1] J. A. van Dam, Yu. V. Nazarov, E. P. A. M. Bakkers, S. De Franceschi, and L. P. Kouwenhoven, Nature (London) **442**, 667 (2006).

[2] A. Yu. Kasumov, R. Deblock, M. Kociak, B. Reulet, H. Bouchiat, I. I. Khodos, Yu. B. Gorbatov, V. T. Volkov, C. Journet, and M. Burghard, Science **284**, 1508 (1999); A. F. Morpurgo, J. Kong, C. M. Marcus, and H. Dai, *ibid.* **286**, 263 (1999); M. R. Buitelaar, T. Nussbaumer, and C. Schönenberger, Phys. Rev. Lett. **89**, 256801 (2002); J.-P. Cleuziou, W. Wernsdorfer, V. Bouchiat, T. Ondarçuhu, and M. Monthioux, Nat. Nanotechnol. **1**, 53 (2006).

[3] M. R. Buitelaar, W. Belzig, T. Nussbaumer, B. Babić, C. Bruder, and C. Schönenberger, Phys. Rev. Lett. **91**, 057005 (2003).

[4] A. Y. Kasumov, K. Tsukagoshi, M. Kawamura, T. Kobayashi, Y. Aoyagi, K. Senba, T. Kodama, H. Nishikawa, I. Ikemoto, K. Kikuchi, V. T. Volkov, Y. A. Kasumov, R. Deblock, S. Guéron, and H. Bouchiat, Phys. Rev. B **72**, 033414 (2005).

[5] H. I. Jorgensen, K. Grove-Rasmussen, T. Novotný, K. Flensberg, and P. E. Lindelof, Phys. Rev. Lett. **96**, 207003 (2006).

[6] J. Xiang, A. Vidan, M. Tinkham, R. M. Westervelt, and C. M. Lieber, Nat. Nanotechnol. **1**, 208 (2006).

[7] P. Jarillo-Herrero, J. A. van Dam, and L. P. Kouwenhoven, Nature (London) **439**, 953 (2006).

[8] A. Eichler, M. Weiss, S. Oberholzer, C. Schönenberger, A. L. Yeyati, J. C. Cuevas, and A. Martín-Rodero, Phys. Rev. Lett. **99**, 126602 (2007).

[9] T. Sand-Jespersen, J. Paaske, B. M. Andersen, K. Grove-Rasmussen, H. I. Jorgensen, M. Aagesen, C. B. Sorensen, P. E. Lindelof, K. Flensberg, and J. Nygard, Phys. Rev. Lett. **99**, 126603 (2007).

[10] E. N. Bratus, V. S. Shumeiko, and G. Wendin, Phys. Rev. Lett. **74**, 2110 (1995); D. Averin and A. Bardas, *ibid.* **75**, 1831 (1995); J. C. Cuevas, A. Martín-Rodero, and A. L. Yeyati, Phys. Rev. B **54**, 7366 (1996).

[11] Å. Ingerman, G. Johansson, V. S. Shumeiko, and G. Wendin, Phys. Rev. B **64**, 144504 (2001); J. Lantz, V. S. Shumeiko, E. Bratus, and G. Wendin, *ibid.* **65**, 134523 (2002).

[12] A. L. Yeyati, J. C. Cuevas, A. López-Dávalos, and A. Martín-Rodero, Phys. Rev. B **55**, R6137 (1997).

[13] G. Johansson, E. N. Bratus, V. S. Shumeiko, and G. Wendin, Phys. Rev. B **60**, 1382 (1999).

[14] L. Glazman and K. A. Matveev, JETP Lett. **49**, 659 (1989); A. V. Rozhkov and D. P. Arovas, Phys. Rev. Lett. **82**, 2788 (1999); E. Vecino, A. Martín-Rodero, and A. L. Yeyati, Phys. Rev. B **68**, 035105 (2003); F. Siano and R. Egger, Phys. Rev. Lett. **93**, 047002 (2004); M. S. Choi, M. Lee, K. Kang, and W. Belzig, Phys. Rev. B **70**, 020502(R) (2004); C. Karrasch, A. Oguri, and V. Meden, *ibid.* **77**, 024517 (2008).

[15] K. Kang, Phys. Rev. B **57**, 11891 (1998); Physica E (Amsterdam) **5**, 36 (1999); S. Y. Liu and X. L. Lei, Phys. Rev. B **70**, 205339 (2004).

[16] Y. Avishai, A. Golub, and A. D. Zaikin, Phys. Rev. B **63**, 134515 (2001).

[17] F. S. Bergeret, A. L. Yeyati, and A. Martín-Rodero, Phys. Rev. B **74**, 132505 (2006); Y. Avishai, A. Golub, and A. D. Zaikin, *ibid.* **67**, 041301(R) (2003).

[18] A. L. Yeyati, A. Martín-Rodero, and E. Vecino, Phys. Rev. Lett. **91**, 266802 (2003).

[19] T. Fujii and K. Ueda, J. Phys. Soc. Jpn. **74**, 127 (2005).

[20] M. Hamasaki, Condens. Matter Phys. **10**, 235 (2007).

[21] R. Egger and A. O. Gogolin, Phys. Rev. B **77**, 113405 (2008).

[22] A. Zazunov, R. Egger, C. Mora, and T. Martin, Phys. Rev. B **73**, 214501 (2006).

[23] B. Horváth, B. Lazarovits, O. Sauret, and G. Zaránd, arXiv:0712.0296 (unpublished).

[24] G. Baym and L. P. Kadanoff, Phys. Rev. **124**, 287 (1961); **127**, 1391 (1962).

[25] S. Hershfield, J. H. Davies, and J. W. Wilkins, Phys. Rev. B **46**, 7046 (1992).

[26] A. Levy Yeyati, J. C. Cuevas, and A. Martín-Rodero, Phys. Rev. Lett. **95**, 056804 (2005).